

## DYNAMICAL CONFIRMATION OF SDSS WEAK LENSING SCALING LAWS

TIMOTHY A. MCKAY<sup>1,10</sup>, ERIN SCOTT SHELTON<sup>1</sup>, DAVID JOHNSTON<sup>2,10</sup>, EVA K. GREBEL<sup>3</sup>, FRANCISCO PRADA<sup>3</sup>, HANS-WALTER RIX<sup>3</sup>, NETA A. BAHCALL<sup>4</sup>, J. BRINKMANN<sup>5</sup>, ISTVÁN CSABAI<sup>6,7</sup>, MASATAKA FUKUGITA<sup>8</sup>, D.Q. LAMB<sup>2</sup>, DONALD G. YORK<sup>2,9</sup>*Accepted for publication in ApJ letters*

## ABSTRACT

Galaxy masses can be estimated by a variety of methods; each applicable in different circumstances, and each suffering from different systematic uncertainties. Confirmation of results obtained by one technique with analysis by another is particularly important. Recent SDSS weak lensing measurements of the projected-mass correlation function reveal a linear relation between galaxy luminosities and the depth of their dark matter halos (measured on  $260 h^{-1}$  kpc scales). In this work we use an entirely independent dynamical method to confirm these results. We begin by assembling a sample of 618 relatively isolated host galaxies, surrounded by a total of 1225 substantially fainter satellites. We observe the mean dynamical effect of these hosts on the motions of their satellites by assembling velocity difference histograms. Dividing the sample by host properties, we find significant variations in satellite velocity dispersion with host luminosity. We quantify these variations using a simple dynamical model, measuring  $M_{260}^{dyn}$  a dynamical mass within  $260 h^{-1}$  kpc. The appropriateness of this mass reconstruction is checked by conducting a similar analysis within an N-body simulation. Comparison between the dynamical and lensing mass-to-light scalings shows reasonable agreement, providing some quantitative confirmation for the lensing results.

*Subject headings:* galaxies: fundamental parameters, structure, mass function, halos

## 1. INTRODUCTION

Mass clustered around galaxies distorts the local space-time, bending light rays which pass near them and inducing distortions in the images of more distant galaxies. Observation of these distortions enables weak lensing measurements of the projected-mass correlation function (PMCF: Brainerd, Blandford and Smail (1996); Fischer et al. (2000); Wilson, Kaiser, Luppino, & Cowie (2001); Hoekstra, Yee, & Gladders (2001)). Recent measurements of the PMCF in fields drawn from the Las Campanas Redshift Survey (Smith, Bernstein, Fischer, & Jarvis 2001) and the Sloan Digital Sky Survey (McKay, et al. (2002): hereafter M02) reveal an approximately linear correlation between the luminosity of  $L > L_*$  galaxies and the depth of the dark matter potential wells in which they reside. This close connection is not particularly surprising in a modern picture of galaxy formation (Seljak 2000; Guzik & Seljak 2001), though it requires rather uniform integrated star formation efficiency across halos of a range of masses.

The weak lensing effects induced by galaxies are very small; peak distortions of background galaxies in the SDSS are only 0.5%. In addition, quantitative interpretation of

the lensing results requires an accurate understanding of lens geometries. It is important to quantitatively confirm these lensing results by independent methods.

In this work we briefly examine galaxy mass-to-light scalings with an independent dynamical method. We extract a sample of ‘host’ galaxies surrounded by systems of ‘satellites’ from data collected by the Sloan Digital Sky Survey. Host galaxies typically have few satellites, making it impractical to measure their masses individually. By combining satellites from many hosts of similar luminosity, we measure the mean velocity field around the hosts. The method is analogous to the ‘stacking’ of galaxies used in lensing measurements of the PMCF. It is closely related to the satellite galaxy analyses of Zaritsky, Smith, Frenk, & White (1993) and Zaritsky & White (1994).

## 2. DATA, AND THE SELECTION OF HOST AND SATELLITE GALAXIES

Data for this study are drawn from Sloan Digital Sky Survey<sup>11</sup>: a combined imaging and spectroscopic survey of  $10^4 \text{ deg}^2$  in the North Galactic Cap, and a smaller, deeper region in the South. The imaging survey is carried out in drift-scan mode in five SDSS filters ( $u, g, r, i, z$ ) to a lim-

<sup>1</sup> University of Michigan, Department of Physics, 500 East University, Ann Arbor, MI 48109

<sup>2</sup> The University of Chicago, Department of Astronomy and Astrophysics, 5640 S. Ellis Ave., Chicago, IL 60637

<sup>3</sup> Max-Planck-Institut für Astronomie, Königstuhl 17, D-69117 Heidelberg, Germany

<sup>4</sup> Princeton University Observatory, Princeton, NJ 08544

<sup>5</sup> Apache Point Observatory, P.O. Box 59, Sunspot, NM 88349-0059

<sup>6</sup> Department of Physics and Astronomy, The Johns Hopkins University, 3701 San Martin Drive, Baltimore, MD 21218

<sup>7</sup> Department of Physics of Complex Systems, Eötvös University, Pázmány Péter sétány 1

<sup>8</sup> University of Tokyo, Institute for Cosmic Ray Reserach, Kashiwa, 2778582, Japan

<sup>9</sup> The University of Chicago, Enrico Fermi Institute, 5640 S. Ellis Ave., Chicago, IL 60637

<sup>10</sup> Center for Cosmological Physics, University of Chicago, 5640 S. Ellis Ave., Chicago, IL 60637

<sup>11</sup> www.sdss.org

iting magnitude of  $r < 22.5$  (Fukugita et al. 1996; Gunn et al. 1998). The spectroscopic survey targets a ‘main’ sample of galaxies with  $r < 17.8$  and a median redshift of  $z \sim 0.1$  (Strauss, et al. 2001). Velocity errors in the redshift survey are  $\sim 30$  km/s. For more details of the SDSS see York et al. (2000) and Stoughton et al. (2002). For this study we extract from the SDSS main galaxy sample a catalog of 102,922 galaxies with accurately measured redshifts in a range from  $z=0.01$  to  $z=0.2$ .

Potential host galaxies must pass an isolation cut: they must be at least two times more luminous than any galaxy within a projected distance of  $2 h^{-1}$  Mpc and a velocity window of  $\pm 1000$  km/s. Around each such host, we select as possible satellites all galaxies at least four times fainter than the host (1.5 magnitudes), within a projected distance of  $500 h^{-1}$  kpc, and within a velocity window of  $\pm 1000$  km/s. Combining the requirement of faint satellites with the magnitude limit of the SDSS spectroscopic survey limits our host galaxies to  $r < 16.3$ .

There are 13,737 galaxies with  $r < 16.3$  in the sample. Of these, 618 are both isolated and have at least one faint satellite. Most of the remainder fail the isolation cut. The total number of satellites is 1225. While the mean number of satellites around each host is only two, there are host galaxies with as many as 19 satellites. An object with this many satellites is clearly more a group with a dominant central galaxy than a galaxy with a few satellites. We remove these by requiring that the combined luminosity of the satellites be less than the luminosity of the host. All but 5 of the host systems pass this cut. Absolute magnitude distributions of host and satellite galaxies are shown in Figure 1. Many still fainter satellites exist; we are prevented from identifying them by the magnitude limit of the SDSS spectroscopic survey.

To reveal the mix of host galaxy types, we divide galaxies into early (redder) and late (bluer) types using  $u-r$  color as described in Strateva, et al. (2001). The  $u-r$  distribution for host and satellite galaxies is shown in the lower right panel of Figure 1. Overall the host galaxies are 75% early and 25% late types. It is important to stress that this division of early and late is luminosity dependent in a way which is strongly color dependent. In  $u$ , late types constitute 25% of galaxies at all luminosities, while in  $z$ , late types are  $> 50\%$  of low luminosity galaxies, and  $< 5\%$  of high luminosity galaxies. This variation in the morphological mix with luminosity complicates comparison of these results to the M02 lensing results in the bluer bands, where early and late type galaxies have substantially different mass-to-light ratios.

### 3. DEPENDENCE OF SATELLITE DYNAMICS ON HOST LUMINOSITY

To examine the relationship between satellite dynamics and host galaxy luminosity, we bin systems by host luminosity, then examine the host-satellite velocity difference histograms for each luminosity bin. All luminosities are based on SDSS Petrosian magnitudes,  $k$ -corrected in the manner described in Blanton et al. (2001). An increase in the dispersion of satellite motions with host luminosity is clearly detected.

We quantify this variation by fitting the velocity difference histogram in each luminosity bin to the sum of a

Gaussian plus a constant, where the constant term represents the contribution due to random interlopers not physically associated with the host galaxy. The Gaussian widths fit to these distributions ( $\sigma_r$ ) are direct measures of the velocity dispersion characteristic of satellites for host galaxies in each luminosity bin. While models of satellite motions (White & Zaritsky 1992) suggest that the line of sight velocity dispersion of satellites may be non-Gaussian, our measured profiles are well fit by these models. Errors quoted for these Gaussian fits include the degeneracy between peak height and width.

### 4. MASS MODELING

To compare these results to the weak lensing results of M02, we need to determine model masses for each luminosity bin. The M02 lensing results quantify mass-to-light scalings by measuring  $M_{260}$ ; the mass inferred by fitting a singular isothermal sphere model to the observed density contrast within a radius of  $260 h^{-1}$  kpc. We calculate here a very similar parameter,  $M_{260}^{dyn}$ .

To derive this parameter we adopt a Jeans approach. This approach is unlikely to represent the situation in detail, as the dynamical times for satellites at projected separations of  $500 h^{-1}$  kpc approach the Hubble time. We address this concern briefly by reference to N-body simulations in the following section. We begin with the relation (Binney and Tremaine 1987):

$$\frac{GM(r)}{r} = -\overline{v_r^2} \left( \frac{\partial \ln \nu}{\partial \ln r} + \frac{\partial \ln \overline{v_r^2}}{\partial \ln r} + 2\beta \right) \quad (1)$$

where  $r$  is the radius at which we measure the mass,  $\overline{v_r^2}$  is the average radial velocity of satellites squared,  $\nu(r)$  is the number density of satellites as a function of radius, and  $\beta$  is the velocity anisotropy

$$\beta = 1.0 - \frac{\overline{v_\theta^2}}{\overline{v_r^2}} \quad (2)$$

By measuring the projected number density of satellites as a function of radius we determine  $\nu(r) \propto r^{-2.1}$ . Measurements of  $\sigma_r$  in apertures from 100 to  $500 h^{-1}$  kpc show no significant variation, implying that the second term in the parentheses of Equation 1 is zero. We assume that the velocity anisotropy  $\beta=0$ . If this is incorrect, the masses determined here will be biased by a factor of  $\sim (1.0 - \beta)$ . Finally, we assume that our measured  $\sigma_r^2$ , the mean square line of site velocity of all satellites within a projected distance of  $500 h^{-1}$  kpc of the host, is equal to  $\overline{v_r^2}$ . These are significant assumptions, which we test below by simulation.

With these assumptions, our mass estimator reduces to the simple form:

$$M_{260}^{dyn} = \frac{2.1 \times r \times \overline{v_r^2}}{G} \quad (3)$$

where  $r$  is the  $260 h^{-1}$  kpc radius to which we integrate the mass, and  $\overline{v_r^2}$  is the one dimensional RMS satellite velocity.

### 5. COMPARISON TO GIF SIMULATIONS

A variety of assumptions were made to arrive at Equation 3. It is possible that one or more of these assumptions introduces systematic error. In addition, it is desirable

to relate the mass estimator  $M_{260}^{dyn}$  to theoretically favored quantities like  $M_{200}$ . As a first test, we conduct a parallel analysis within a simulated universe, extracting the observables used in our analysis from the simulation. By reconstructing masses in the simulation using  $M_{260}^{dyn}$ , and comparing these to  $M_{200}$ , it is possible to both test the validity of  $M_{260}^{dyn}$  and understand its relationship to  $M_{200}$ .

To conduct this test we turn to the GIF simulations of Kauffman, et al. (1999). GIF combines N-body simulations of the evolution of dark matter clustering with a semianalytic galaxy modeling scheme, including gas cooling, star formation, feedback from supernovae, and galaxy merging. The end result is a catalog of galaxies with B, V, R, I, and K magnitudes and stellar masses. Peculiar velocities for each galaxy are determined from the N-body simulations. As a result, these velocities have the full structure we might expect to find in the data. The most important limitation of the GIF simulations for this comparison is their relatively low mass resolution. They resolve only the most massive and luminous host galaxies.

To test our analysis of SDSS satellite motions, we conduct a parallel analysis within the GIF simulations. We define as isolated all galaxies which are at least two times brighter than any other galaxy within their halo. We then search these for cases with satellites at least four times fainter. We use the velocity differences between hosts and satellites to populate velocity difference histograms, and sort these by host luminosity, in the same manner used in the SDSS satellite study. As a first check of Equation 3, we use the simulations to check our assumptions about  $\beta$  and the relationship between  $\sigma_r^2$  and  $\overline{v_r^2}$ . We calculate the velocity anisotropy from the simulation, and find  $\beta = 0.06 \pm 0.03$ . We also find the LOS velocity dispersion  $\sigma_r^2 = 1.03 \pm 0.03 \times \overline{v_r^2}$ . While the GIF simulations are not a perfect match to our satellite sample, this provides some support for the assumptions we made in deriving Equation 3.

A more direct approach is to confirm that the data and simulations show a consistent relationship between the observables:  $\sigma_r$  and luminosity. This comparison of the SDSS and GIF  $\sigma_r$  vs. luminosity measurements is shown in Figure 2. The SDSS luminosity measurements are in  $i$ , and the GIF luminosities in Johnson I, but as both are converted to solar luminosities the comparison remains appropriate. Both the SDSS and GIF results are consistent with a simple model in which  $\sigma_r \propto L^{0.5}$ .

Since the GIF simulations provide values for the  $M_{200}$  associated with each halo, we can compare measures of  $M_{260}^{dyn}$  derived from galaxy velocities to  $M_{200}$  within the simulations. This comparison suggests that  $M_{260}^{dyn} \approx 0.7 \times M_{200}$ . It is essential to note that this relation is determined only for the most luminous galaxies, and over only a factor of four in luminosity. While this comparison is limited, it provides some confidence that Equation 3 sensibly relates satellite velocities to masses. A more detailed understanding awaits simulations with higher mass resolution, in which more direct comparisons can be made.

#### 6. MASS-TO-LIGHT SCALINGS AND COMPARISONS TO LENSING RESULTS

The measurements of  $M_{260}^{dyn}$  derived from satellite motions are shown in Figure 3. The relationship between

$M_{260}^{dyn}$  and light in each passband is well fit by a single power law. As observed in M02, these relations are consistent with a power law index of one (constant  $M/L$ ) in all bands except  $u$ , where a flatter relation, with a best fit power law index  $\sim 0.6$  is observed.

To compare these results to the M02 lensing results, we fix the power law index to one, and fit the  $M_{260}^{dyn}$  vs. luminosity data in each band to obtain values for  $M/L$ . Values for these  $M/L$  ratios are given in Figure 3. The dynamical  $M/L$  values are consistent with the lensing values at the  $1\sigma$  level in most bands. They differ most strongly in  $u$  and  $g$ , where M02 suggests results will be very sensitive to the mix of host types.

The masses of  $L_*$  galaxy halos are proportional to light, and  $M/L$  values vary strongly with color. More detailed quantitative comparison of the lensing and dynamical results will only be possible when we can measure more identical samples of hosts and lenses. This is difficult. The magnitude limit of the SDSS spectroscopy biases dynamical studies toward hosts at  $z < 0.05$ , while lens geometries prefer lenses at  $z \sim 0.15$ . Still, the  $M/L$  values derived by independent methods agree reasonably, especially in the redder bands, where differences between the host and lens samples are probably less important.

#### 7. CONCLUSIONS

Recent SDSS weak lensing results (M02) revealed a linear relation between galaxy luminosity and mass on halo scales. To quantitatively test this result, we have measured the relationship between galaxy luminosity and satellite dynamics for a large sample of reasonably isolated host galaxies. We observe a highly significant increase in satellite velocity with host luminosity.

To make direct comparisons to the weak lensing results, we apply a simple mass estimator,  $M_{260}^{dyn}$ , which is closely analogous to the mass modeling used in M02. A first order test of the validity of this model is made by computing it within the GIF simulations. The relationship seen here between  $M_{260}^{dyn}$  and luminosity matches reasonably the relation seen by entirely independent weak lensing methods. This confirms the essential conclusions reached in M02. The luminous and dark components of  $L_*$  galaxies are strongly coupled on  $\sim 200$  kpc scales.

It is unknown whether the scaling relations observed here for super- $L_*$  galaxies apply at lower luminosity. Perhaps the most important future extension of these studies will be to less luminous galaxies. Additional comparison of lensing and dynamical mass estimates will require measurement of more closely related host and lens samples, and more detailed study of the extraction of mass from the observable PMCF and satellite velocity structure.

The Sloan Digital Sky Survey (SDSS) is a joint project of The University of Chicago, Fermilab, the Institute for Advanced Study, the Japan Participation Group, The Johns Hopkins University, Los Alamos National Laboratory, the Max-Planck-Institute for Astronomy (MPIA), the Max-Planck-Institute for Astrophysics (MPA), New Mexico State University, Princeton University, the United States Naval Observatory, and the University of Washington. Apache Point Observatory, site of the SDSS tele-

scopes, is operated by the Astrophysical Research Consortium (ARC).

Funding for the project has been provided by the Alfred P. Sloan Foundation, the SDSS member institutions, the National Aeronautics and Space Administration, the National Science Foundation, the U.S. Department of Energy, the Japanese Monbukagakusho, and the Max Planck Soci-

ety. The SDSS Web site is <http://www.sdss.org/>. Timothy McKay and Erin Sheldon gratefully acknowledge support from NSF PECASE grant AST 9708232. We thank the GIF team for making their simulations publically available, and acknowledge Simon White and the anonymous referee for constructive suggestions.

#### REFERENCES

- Binney, J., and Tremaine, S., 1987, *Galactic Dynamics* (Princeton, NJ: Princeton University Press)
- Blanton, M. R. et al. 2001, *AJ*, 121, 2358
- Brainerd, T. G., Blandford, R. D. and Smail, I. 1996, *ApJ*, 466, 623
- Eisenstein, D., et al. 2001, accepted for publication in *AJ*
- Fischer, P. et al. 2000, *AJ*, 120, 1198
- Fukugita, M., Ichikawa, T., Gunn, J. E., Doi, M., Shimasaku, K., & Schneider, D. P. 1996, *AJ*, 111, 1748
- Gunn, J. E. et al. 1998, *AJ*, 116, 3040
- Guzik, J. & Seljak, U.; 2001, *MNRAS*, 321, 439
- Hoekstra, H., Yee, H., and Gladders, M., 2001, submitted to *ApJ*, also astro-ph/0107413
- Kauffman, G., Kolberg, J., Diaferio, A., & White, S.D.M., 1999, *MNRAS*, 303, 188
- McKay, T., et al., 2002, submitted to *ApJ*, also astro-ph/0108013
- Seljak, U., 2000, *MNRAS* 318, 203
- Smith, D. R., Bernstein, G. M., Fischer, P., & Jarvis, M. 2001, *ApJ*, 551, 643
- Stoughton, C. et al. 2002, *AJ*, 123, 485
- Strateva, I., et al. 2001, accepted for publication in *AJ*, also astro-ph/0107201
- Strauss, M., et al., in preparation
- York, D. G. et al. 2000, *AJ*, 120, 1579
- White, S. D. M. & Zaritsky, D. 1992, *ApJ*, 394, 1
- Wilson, G., Kaiser, N., Luppino, G. A., & Cowie, L. L. 2001, *ApJ*, 555, 572
- Zaritsky, D. 1992, *ApJ*, 400, 74
- Zaritsky, D., Smith, R., Frenk, C., & White, S. D. M. 1993, *ApJ*, 405, 464
- Zaritsky, D. & White, S. D. M. 1994, *ApJ*, 435, 599

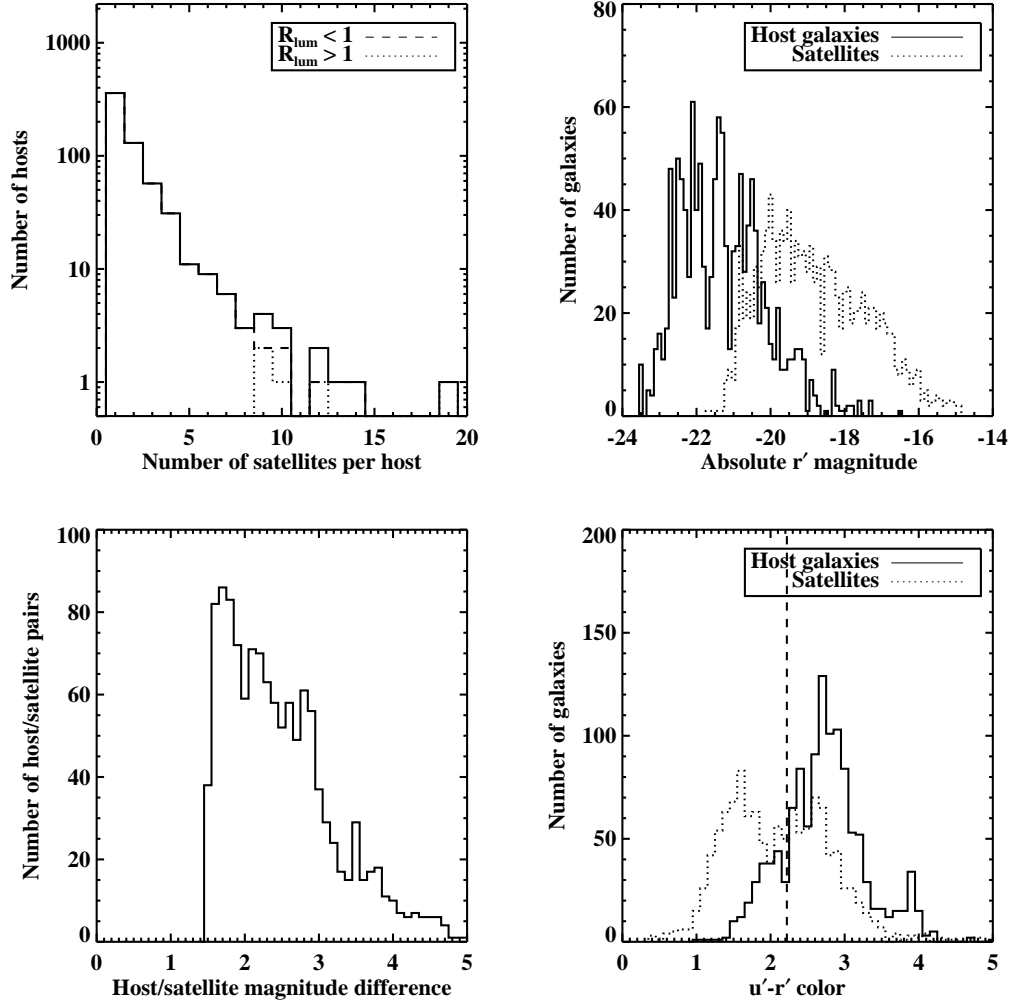


FIG. 1.— The four panels here provide an overview of the host and satellite populations selected by this method. The upper left panel is a histogram of the number of satellites per host. The solid line is the full sample, the dashed (dotted) line is for those systems where the host galaxy is more (less) luminous than the sum of its satellites. The upper right panel shows the absolute  $r$  magnitudes of the hosts and satellites in bins of 0.1 mag (using  $H_0 = 100 h \text{ km s}^{-1} \text{ Mpc}^{-1}$  throughout). The lower left panel shows the distribution of magnitude differences between hosts and satellites. Finally, the lower right shows the distribution of  $u-r$  colors for hosts and satellites. The vertical dashed line in this figure shows the approximate dividing line between early (redder) and late (bluer) type galaxies discussed in Strateva, et al. (2001).

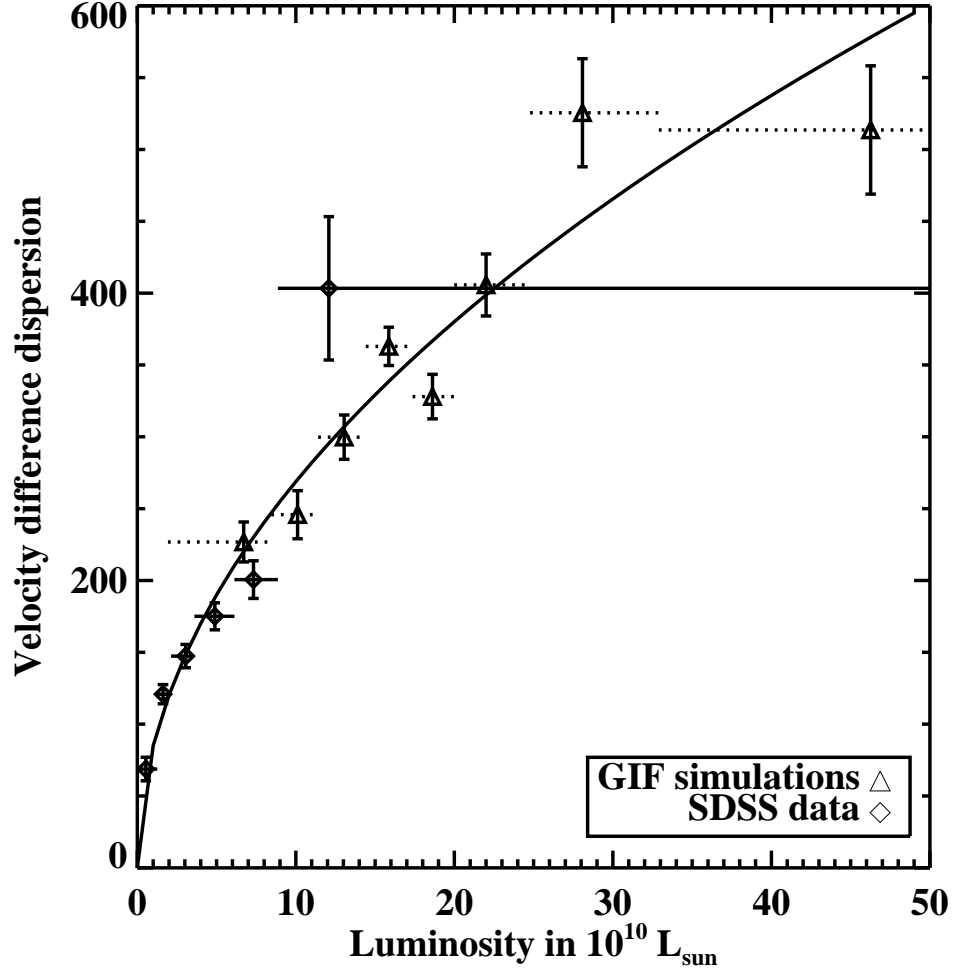


FIG. 2.— This figure compares measurements of satellite velocity dispersion vs. luminosity for real SDSS satellites (diamonds) and simulated GIF satellites (boxes). The two measures are well represented by a single relationship  $\sigma_v \propto L^{0.5}$ . Vertical error bars represent the uncertainties in determination of the satellite velocity dispersion. Horizontal error bars represent the range of host luminosities for each bin. The results from GIF simulations allow us to test the applicability of our mass estimator. The similarity of the simulations and observations at this observable level give some confidence in the comparison.

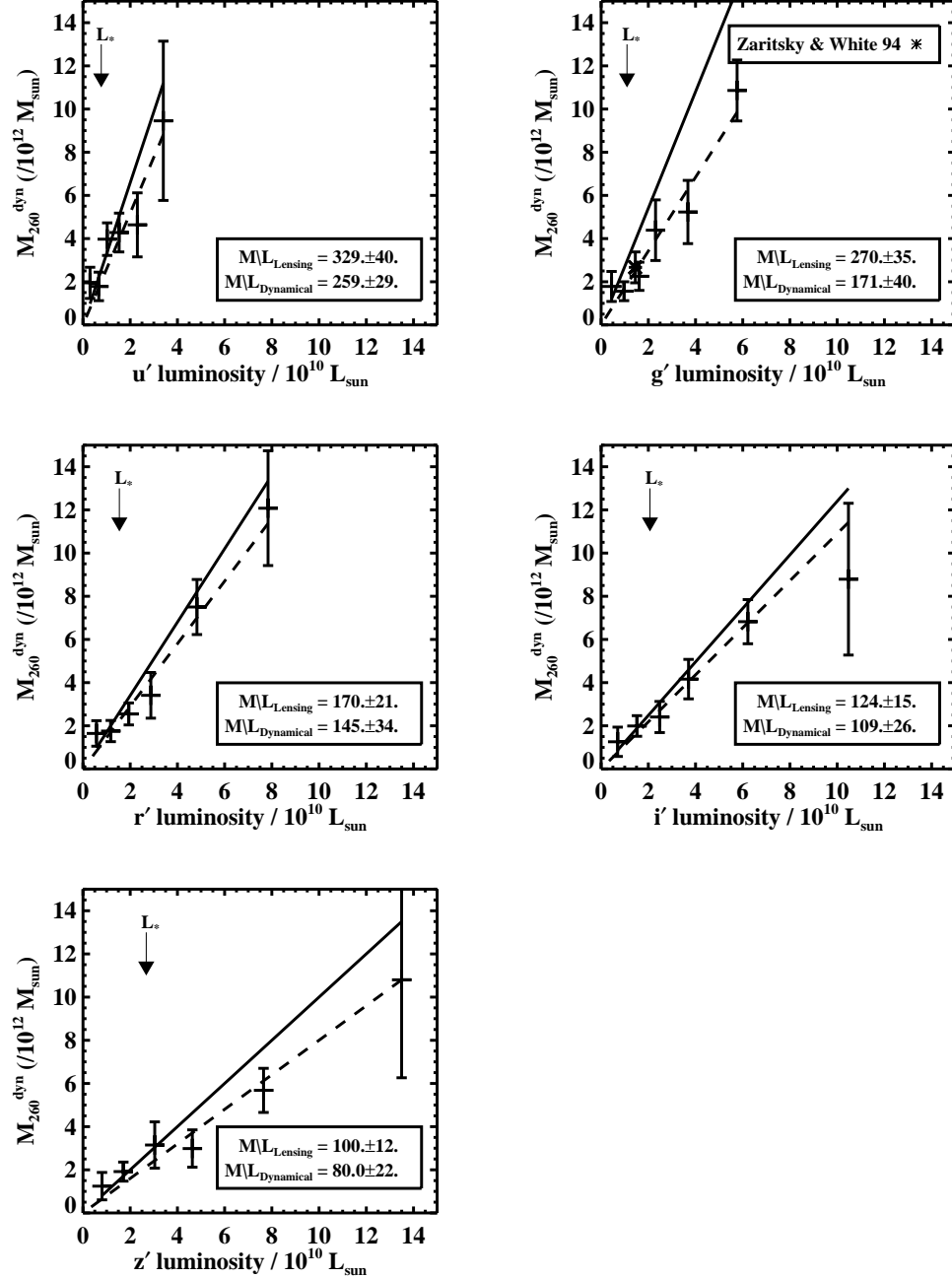


FIG. 3.— This figure shows the relationship between  $M_{260}^{dyn}$  and luminosity in each of the five SDSS bands. In each plot the data points are the  $M_{260}^{dyn}$  estimates for each luminosity bin. In the  $g$  plot, an additional point has been added giving the approximate mass derived from satellite studies of Zaritsky & White (1994), scaled to a radius of  $260 h^{-1}$  kpc assuming isothermality. The vertical arrow in each plot marks the luminosity of an  $L_*$  galaxy in each band. The solid line in each plot represents the best fit lensing  $M/L$  for from M02. The dashed lines represent the best fit constant  $M/L$  model from these dynamical measurements. Note that all five figures are on the same scale. Most of the variation of mass with luminosity is seen for  $L > L_*$  galaxies.